



HAL
open science

Inhibition of the drug efflux activity of Ptch1 as a promising strategy to overcome chemotherapy resistance in cancer cells

Sandra Kovachka, Giuliano Mallocci, Méliné Simsir, Paolo Ruggerone, Stéphane Azoulay, Isabelle Mus-Veteau

► To cite this version:

Sandra Kovachka, Giuliano Mallocci, Méliné Simsir, Paolo Ruggerone, Stéphane Azoulay, et al.. Inhibition of the drug efflux activity of Ptch1 as a promising strategy to overcome chemotherapy resistance in cancer cells. *European Journal of Medicinal Chemistry*, 2022, 236, pp.114306. 10.1016/j.ejmech.2022.114306 . hal-03845877

HAL Id: hal-03845877

<https://hal.science/hal-03845877>

Submitted on 9 Nov 2022

HAL is a multi-disciplinary open access archive for the deposit and dissemination of scientific research documents, whether they are published or not. The documents may come from teaching and research institutions in France or abroad, or from public or private research centers.

L'archive ouverte pluridisciplinaire **HAL**, est destinée au dépôt et à la diffusion de documents scientifiques de niveau recherche, publiés ou non, émanant des établissements d'enseignement et de recherche français ou étrangers, des laboratoires publics ou privés.

Review for the special issue of European Journal of Medicinal Chemistry on drug candidates targeting multidrug resistance in cancers and infectious disease

Inhibition of the drug efflux activity of P_{tch1} as a promising strategy to overcome chemotherapy resistance in cancer cells

Sandra Kovachka^{1,2}, Giuliano Mallocci³, Méliné Simsir², Paolo Ruggerone³, Stéphane Azoulay¹ and Isabelle Mus-Veteau^{2*}

¹ Université Côte d'Azur, CNRS, ICN, 28 Avenue Valrose, 06108 Nice, CEDEX 2, France. E-mail: stephane.azoulay@univ-cotedazur.fr

² Université Côte d'Azur, CNRS, IPMC, 660 Route des Lucioles, 06560 Valbonne, France. E-mail: mus-veteau@ipmc.cnrs.fr

³ Dipartimento di Fisica, Università di Cagliari, Cittadella Universitaria, I-09042 Monserrato (CA), Italy. E-mail: giuliano.mallocci@dsf.unica.it; paolo.ruggerone@dsf.unica.it

* To whom correspondence should be addressed.

Abstract

The development of inhibitors of key biological mechanisms involved in multidrug resistance (MDR) burden meets an important medical need but still represents a challenging task. Major MDR targets in both bacterial and cancer cells are multidrug efflux systems. Several aspects should be considered in the attempt to design efficient inhibitors of these systems such as toxicity, stability, permeability as a few examples. In order to successfully design promising new compounds, a full understanding of the efflux mechanism is required, from both biological and structural points of view. It is nowadays well established that the success rate in classical drug design and biological evaluation improves when combined with *in silico* methodologies. In this review, we focus on the biological evaluation and molecular mechanistic insights of inhibitors of the drug efflux activity of the Hedgehog receptor Patched1 (Ptch1). Ptch1 is known to be over-expressed in many types of cancers, but its activity and role in the resistance to chemotherapy of cancer cells have been highlighted only recently. Remarkably, due to its peculiar efflux mechanism, inhibition of Ptch1 was shown to be particularly relevant for improving the efficacy of chemotherapy without concomitant toxicity for healthy cells or potential side effects. To date, three compounds have been identified as efficient Ptch1 inhibitors, namely astemizole, methiothepin and panicein A hydroquinone. Due to the chemical and structural differences of these molecules, the hit-to-lead drug design is not straightforward. This review describes how the merging of *in vitro*, *in vivo* and *in silico* studies provides molecular details that could contribute to the rational design of new Ptch1 inhibitors.

Key words: Resistance to chemotherapy, Multidrug efflux pump, Ptch1, Hedgehog signaling, drug efflux pump inhibitors

1. Introduction

Despite the major progresses in biomedical research and the development of novel therapeutic strategies, cancer is still among the dominant causes of death worldwide. According to estimates from the World Health Organization (WHO) in 2015, cancer is the first or second leading cause of death before age 70 in 91 of 172 countries, and it ranks third or fourth in an additional 22 countries. Worldwide, 19.3 million estimated new cancer cases occurred in 2020 with almost 10.0 million cancer deaths (Sung et al. 2021). Even though there are several different methods of cancer treatments, including radiation therapy, surgery, immunotherapy, endocrine therapy, and gene therapy, chemotherapy remains the most common method of cancer healing. However, statistical data shows that over 90% mortality of cancer patients is attributed to drug resistance responsible for the decrease of responsiveness to classical and targeted chemotherapies. The resistance mechanism is the result of combined actions of multiple factors and pathways such as drug efflux, increased DNA damage repair, reduced apoptosis, modification or alteration of drug active target proteins, transformation of epithelial cells to mesenchymal cells and hypoxia (Balzerano et al. 2021, Bukowski et al. 2020).

A key feature of cancer biology is its intratumor heterogeneity characterized by genetic and epigenetic variability of somatic cells. The presence of genomic diversity within a single tumor was described for the first time in 1958 (Huxley, 1958), and demonstrated later using single cell sequencing and sub-clonal tumor-region-specific genotyping (Johnson et al. 2014). This study showed that from 0 to over 8000 different coding mutations exist within the same primary tumor or between primary and metastatic stages. Such heterogeneity underlies the lethal outcome of cancer, therapeutic failure, and drug resistance. Despite initial therapeutic responsiveness, treatment can induce a bottleneck in which the death of drug-sensitive cells is counteracted by a massive outgrowth of resistant cells (Prieto-Vila et al. 2017, Mikubo et al. 2021).

Therefore, one of the major challenges in the clinical management of cancer is resistance to chemotherapeutics. Multidrug resistance (MDR) has been intensively studied, and drug efflux induced by the overexpression of ATP-binding cassette (ABC) transporters has been considered as the most prominent underlying mechanism for MDR (Ozben 2006). Since the discovery of the P-glycoprotein (Pgp or MDR1) over 35 years ago, some studies have linked ABC transporter expression to poor outcome in several cancer types, leading to the development of transporter inhibitors to overcome MDR (Wang et al. 2021). At least three generations of MDR1 inhibitors have been tested in clinical trials (Kathawala et al. 2015). The first and second

generation included inhibitors such as verapamil, cyclosporin and valsopar. All these compounds failed in clinical trials due to lack of potency, off-target effects or toxicity issues. More recently, a third generation of inhibitors have been designed, including drugs such as elacridar, zosuquidar and tariquidar, that have proven to be ineffective.

Members of the ABC superfamily transport toxins, sugars, amino acids, nucleotides and metabolites out of cells, and protect cells against toxic molecules, including drugs with very different chemical structures (Cree and Charlton, 2017). Thus, ABC transporters are particularly important for the functioning of healthy cells, and that is why, to date, no inhibitors of ABC transporters have obtained approval from FDA due to their low efficacy or toxicity issues (Kathawala et al. 2015, Robey et al. 2018).

Therefore, treatment able to overcome chemotherapy resistance and thus eliminate resistant cancer cells responsible for the relapse and metastases (also called persistor cells) is still an unmet, urgent, medical need.

2. Role of the Hedgehog receptor Ptch1 in chemotherapy resistance

2.1 Hedgehog signaling in cancers

The Hedgehog (Hh) signaling pathway controls cell differentiation and proliferation. It plays a crucial role during embryonic development, and, in adulthood, it is involved in stem cell homeostasis and tissue regeneration. Hh signaling is also involved in cancer development, progression, and metastasis. In the resting state, the 12-pass transmembrane receptor Patched (Ptch1 in mammals) suppresses the activity of Smoothed (Smo), a GPCR-like molecule. In mammals, three ligands, Desert hedgehog (Dhh), Indian hedgehog (Ihh) or Sonic hedgehog (Shh), activate the canonical Hh signaling by interacting with Ptch1 and inducing its internalization and degradation, which relieves its inhibitory effect on Smo. Each ligand promotes tissue-specific and highly regulated activation of the Hh signaling pathway. Activated Smo signals to the cytoplasm and causes activation of zinc-finger transcription factors Gli that control the transcription of Hh target genes, including Fox, Myc, Ptch1, Hhip, Snail, Nanog, Sox2 and cyclin D, that are involved in cell development, differentiation, epithelial mesenchymal transition (EMT), and stem cell maintenance. In mature adult cells, Hh signaling remains in an inactive state. Its activation is required for tissue development and homeostasis and has a significant role in the maintenance of pluripotent and somatic stem cell populations, and in tissue repair (see Sigafos et al. 2021 for a recent review).

Aberrant activation of Hh signaling has been observed in many cancers (Scale and de Sauvage 2009, Xie et al. 2019, Jeng et al. 2020). A role of the Hh pathway in chemoresistance was reported notably in gastrointestinal cancers (Liang et al. 2021), in oral squamous cell carcinoma (Lu et al 2020), in lung cancer (Giroux-Leprieur et al. 2018) and in Non-Small Cell Lung Carcinoma (NSCLC) Cells (Liu et al. 2020).

2.2 Overexpression of *Ptch1* in cancers

The Hh receptor *Ptch1*, whose expression is induced upon activation of the Hh pathway, is overexpressed in many cancers (see the Human Protein Atlas website <http://www.proteinatlas.org/ENSG00000185920-PTCH1/cancer> (Fig.1), and Hasanovic and Mus-Veteau 2018 for a review).

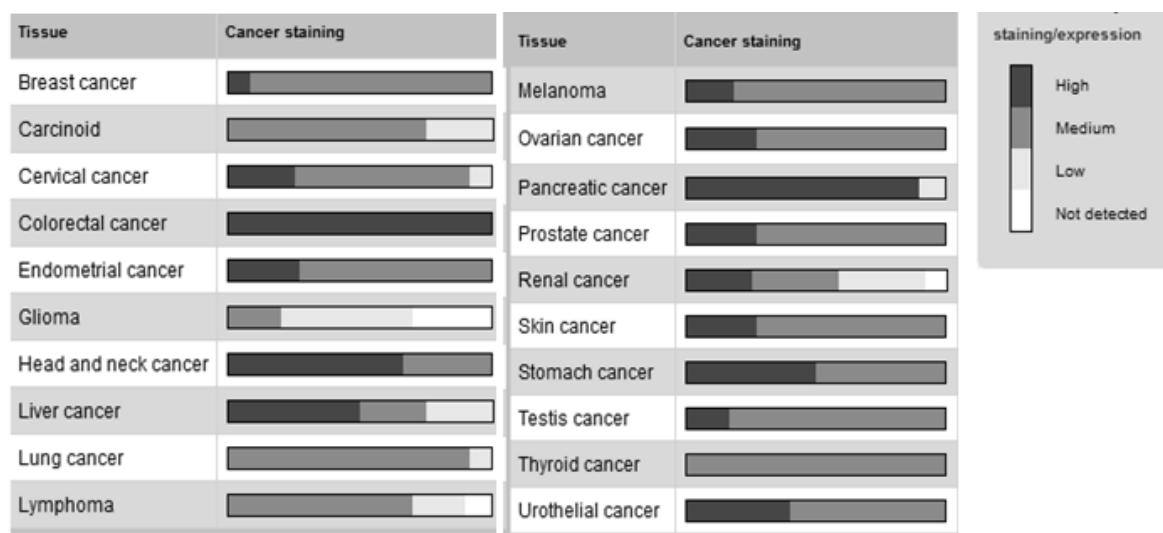


Figure 1. *Ptch1* protein level in cancers (from the Protein Atlas web site). In order to provide an overview of *Ptch1* expression patterns, images of tissues stained by immunohistochemistry have been manually annotated by a specialist followed by verification by a second specialist. Annotation of each different cancer tissue was performed using fixed guidelines for classification of immunohistochemical results. Basic annotation parameters include an evaluation of staining intensity (not detectable, low, medium or high), and fraction of patients with no detectable, low, medium or high staining intensity. For example, 11 of 11 melanoma patients show high/medium expression of *Ptch1* (high: 2, medium: 9, low: 0, not detected: 0).

Ptch1 has been shown to be present in primary tumor samples from all the adrenocortical carcinoma patients of a cohort (Hasanovic et al. 2018), and in Merkel cell carcinoma (Gambichler et al. 2021). The overexpression of *Ptch1* in patients with hepatocellular carcinoma (HCC) was described, and it was suggested that expression of *Ptch1* mRNA in HCC tissues is a potential biomarker to predict post resection disease recurrence (Jeng et al. 2013 and 2019). *Ptch1* has been proposed to be an early marker for gastric and thyroid cancers (Saze et al. 2012, Xu et al. 2012).

Several studies reported the overexpression of Ptch1 in breast cancers as compared with respective normal mammary tissues and a significant correlation of Ptch1 upregulation with invasiveness (lymph node metastasis), advanced cancer stages and more aggressive tumor behavior (Im et al. 2013, Jeng et al. 2013, Riaz et al. 2018). High Ptch1 protein levels were also observed in the metastases of all the 365 melanoma patients of a cohort from The Cancer Genome Atlas (TCGA) and correlated with poor prognosis (Signetti et al. 2020). Moreover, the upregulation of Ptch1 in pancreatic ductal adenocarcinoma was reported to be associated with a trend toward decreased patient survival (Mohelnikova-Duchonova et al. 2017). Likewise, high Ptch1 RNA expression was detected in 64% of high-grade endometrial stromal sarcoma (Momeni-Boroujeni et al. 2021).

Abnormal Hh signaling activation and Ptch1 upregulation were reported in cells exhibiting resistance to chemotherapy such as cancer stem cells or tumor-initiating cells (Cochrane et al. 2015). As an example, elevated expression of Ptch1 was described in the residual gastric cancer cells following chemotherapy treatment with cisplatin and was associated with poor survival in the gastric cancer patients who underwent chemotherapy (Yu et al. 2017). Moreover, high Ptch1 levels were detected in 76% of biopsy specimens from esophageal squamous cell carcinoma patients treated with chemotherapy. Interestingly, significant associations were observed between high Ptch1 and large tumor size / progression, and an incomplete response to chemotherapy, suggesting that high expression of Ptch1 may be associated with resistance to chemotherapy in oesophageal squamous cells carcinoma (Zhu et al. 2011). Furthermore, a recent study described that the upregulation of Ptch1 may be a prognostic marker for relapse in high-risk prostate cancer patients (Gonnissen et al. 2018).

2.3 Role of Ptch1 in cholesterol and drug efflux

Human Ptch1 is an integral membrane protein of 1450 amino acids with 12 transmembrane domains and 2 large extracellular domains. Ptch1 has a sterol sensing domain (SSD) and a large non-structured intracellular domain like the Niemann Pick C1 protein (NPC1). It belongs to the Resistance-Nodulation-Division (RND) superfamily which also includes efflux pumps mostly of bacterial origin (Simsir and Mus-Veteau 2020). RND transporters can extrude a wide variety of substrates such as sterols, lipids, bile salts, fatty acids, and metal ions, as well as lipophilic drugs, and are involved in drug resistance (Nikaido 2018).

Ptch1 was shown to transport cholesterol in 2011 (Bidet et al. 2011), and this cholesterol transport activity of Ptch1 was recently confirmed by structural data (Gong et al. 2018, Qi et al.

2018, Zhang et al. 2018). This way, Ptch1 decreases the intracellular cholesterol concentration around Smo and prevents Smo stabilization at the plasma membrane. When Shh binds to Ptch1, it induces Ptch1 internalization, and the inhibition of the cholesterol efflux. The increase of the cholesterol level allows the stabilization of Smo at the plasma membrane and the activation of Hh signaling (Hasanovic and Mus-Veteau 2018). This explains why cholesterol was often reported to control / regulate Hh signaling (Radhakrishnan et al. 2020, Petrov et al. 2020).

Interestingly, Bidet and colleagues showed for the first time that Ptch1 is a multidrug transporter involved in the resistance of cancers to chemotherapy (Bidet et al. 2012). They expressed human Ptch1 in the plasma membrane of the yeast *Saccharomyces cerevisiae*, and they observed that the expression of Ptch1 conferred to yeast the ability to grow in the presence of chemotherapeutic agents such as doxorubicin, methotrexate or temozolomide, and that yeasts expressing Ptch1 were able to expel more doxorubicin than control yeasts (Bidet et al. 2012). More recent studies reported that the inhibition of endogenous Ptch1 expression in adrenocortical carcinoma (ACC) and melanoma cells using silencing RNA strongly decreased doxorubicin efflux from these cells indicating that Ptch1 contributes significantly to the chemotherapy resistance in these cells (Hasanovic et al. 2018, Signetti et al. 2020). The role of Ptch1 in chemotherapy resistance was strengthened by the observation that ACC cells rendered resistant to doxorubicin express more Ptch1 than parental cells (Hasanovic et al. 2018).

3. Ptch1 drug efflux activity is specific to cancer cells

Efflux pumps from the RND family transport substrates using as an energy source the proton-motive force, an electrochemical gradient in which the movement of protons drives the export of substrates. In several bacterial RND proteins such as AcrB, whose efflux mechanism has been extensively studied (Tam et al. 2020), three or four charged residues (Asp407, Asp408 and Lys940) have been shown to be involved in the proton relay. This Proton Relay Site (PRS) is located for one part at the highly conserved motif GXXXD from the transmembrane helix 4 (Fig. 2A&B), and for the other part on the transmembrane helix 10 (Fig. 2C) (Murakami et al. 2006). The motif GXXXD is also conserved in the fourth transmembrane helix of Patched efflux pumps (Fig. 2A&B). Bidet and co-workers (2012) showed that mutations in this motif inhibited the efflux of doxorubicin and the drug resistance conferred by human Ptch1 expression to yeast. They also showed that treatment with a decoupling agent inducing the disruption of the proton motive force in yeast inhibited the efflux of doxorubicin and cholesterol

(Bidet et al. 2012). Moreover, the structure of human Ptch1 revealed the presence of a PRS formed by two aspartic acids from the transmembrane helix 4 and one glutamic acid from the transmembrane helix 10 (Qian et al 2019, Simsir and Mus-Veteau 2020) (Fig. 3C).

Taken together, these data strongly suggest that Ptch1 transports cholesterol and drugs out of the cells using the proton motive force like its bacterial homologues. By the way, mutation of the GXXXD motif in Ptch1 leads to the Gorlin syndrome which is a hereditary dominant autosomal disease characterized by the development of basocellular carcinoma (Aszterbaum et al. 1998, Chidambaram et al. 1996, Hahn et al. 1996). There is evidence that this disease could be due to a loss of cholesterol transport activity of Ptch1.

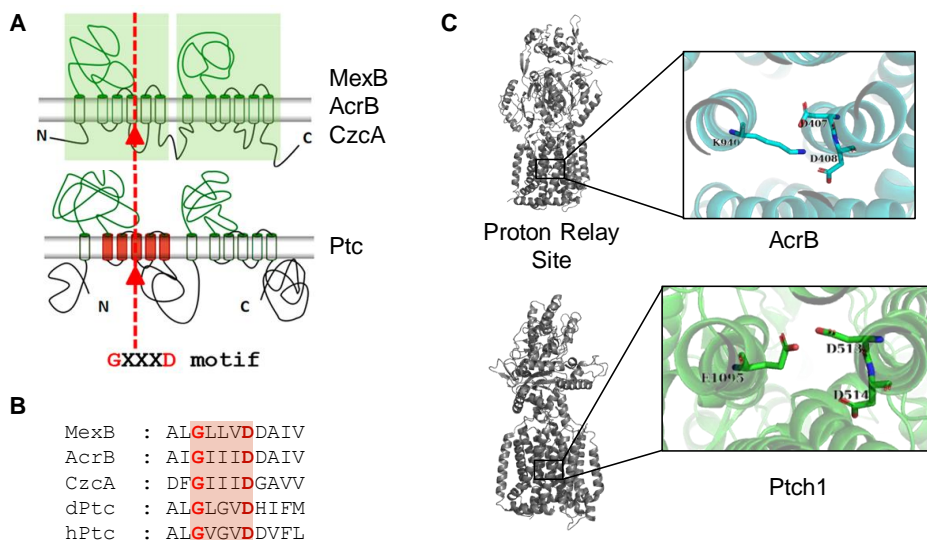


Figure 2. Ptch1 drug efflux activity is driven by proton motive force. A. Schematic representation of the topology of the RND transporters Patched (Ptc) and the bacterial efflux pump MexB, AcrB and CzcA. The sterol sensing domains (SSD) is represented in red and the transmembrane segment containing the highly conserved GXXXD motif is highlighted. B. Sequence alignment of the transmembrane helix 4 containing the GXXXD motif from Patched (Ptc) and from the bacterial efflux pump MexB, AcrB and CzcA. C. Structure of the proton relay sites from AcrB (PDB ID: 2DR6, Murakami et al. 2006), and Ptch1 (PDB ID: 6N7H, Qian et al 2019).

Therefore, to transport cholesterol or drugs, Ptch1 needs the extracellular medium to be more acidic than the intracellular medium. Such a pH gradient does not usually occur for healthy eukaryote cells except in highly proliferating cells, such as cells in development and cancer cells. Indeed, the high glucose consumption of these cells causes a strong production of lactate which is transported out of cells decreasing the extracellular pH. This aerobic glycolysis, also termed the Warburg effect, induces a “reversed pH gradient” which is considered a hallmark of malignant cancers (Heiden et al. 2009, Liberti and Locasale 2016, Damaghi et al. 2013). Therefore, in adults, Ptch1 functions as a drug efflux pump only in cancer cells. This makes

Ptch1 an innovative and highly promising therapeutic target whose inhibition is particularly relevant for improving the effectiveness of anti-cancer treatments without toxicity for healthy cells. In addition, this gives Ptch1 inhibitors a clear advantage over ABC transporter inhibitors in combating resistance to chemotherapy without toxicity to healthy cells or potential side-effects (Fig. 3).

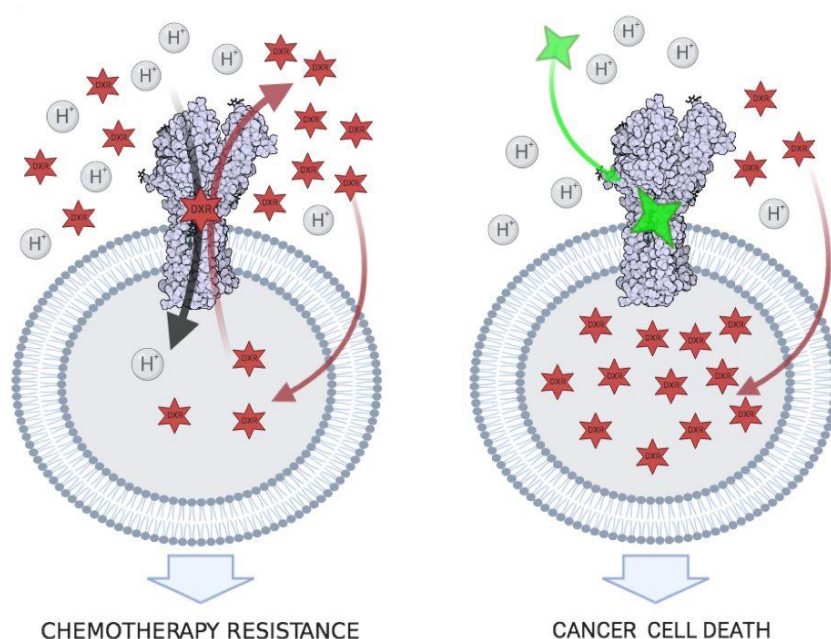


Figure 3. Combination of Ptch1 drug efflux inhibitor and chemotherapy is a potential new therapeutic option to overcome drug resistance of cancer cells. Ptch1 inhibitor (in green) inhibits the doxorubicin (denoted as DXR, in red) efflux activity of Ptch1 (in grey). This allows the concentrations of doxorubicin required to kill cancer cells to be reached and sensitizes resistant cells to chemotherapy.

4. Three inhibitors of Ptch1 drug efflux activity reduce chemotherapy resistance of cancer cells

Screening tests have been developed to identify molecules that inhibit the resistance to doxorubicin (dxr) conferred by human Ptch1 to yeast, and the efflux of dxr by Ptch1 (Fiorini and Mus-Veteau 2016). This led to the discovery of three inhibitors of Ptch1 drug efflux, namely methiothepin, astemizole, and panicein A hydroquinone, whose structure, profiling properties and activity are summarized in Table 1.

4.1 Methiothepin

Methiothepin is a small molecule known as a non-selective 5-HT receptor antagonist with antipsychotic activity (Monachon et al. 1972). This compound was shown to significantly

enhance the cytotoxic, pro-apoptotic, anti-proliferative and anti-clonogenic effects of dxr on adrenocortical carcinoma (ACC) cells by inhibiting the dxr efflux activity of Ptch1. *In vivo* experiments performed on mice bearing human ACC cells xenografts showed that the addition of methiothepin to dxr treatment inhibited tumor growth more significantly than dxr alone by enhancing dxr accumulation in tumors. Notably, these effects were achieved without obvious undesirable side effects and specifically without increasing the amounts of dxr in heart tissues of treated animals (Hasanovic et al. 2018). Interestingly, three chlorinated derivatives of methiothepin (Clorotepine, Zotepine and Clotiapine) marketed for the treatment of schizophrenia (Hrbek et al. 1985) also enhanced the dxr cytotoxicity on ACC cells but with lower efficacy than methiothepin (Hasanovic et al. 2018).

Methiothepin was also shown to overcome the resistance of BRAF^{V600E} melanoma cells by enhancing the cytotoxicity of the targeted chemotherapies against kinases such as vemurafenib (BRAF inhibitor) and trametinib (MEK inhibitor) leading to melanoma cells death. Importantly, the addition of methiothepin to vemurafenib inhibits the migration of resistant melanoma cells more efficiently than vemurafenib alone (Durand et al. 2021). MicroScale Thermophoresis analyses performed on membranes prepared from yeast expressing human Ptch1 confirmed that methiothepin specifically interacts with Ptch1 with a K_d of about 7 μM.

Profiling data and pharmacokinetics study indicate that methiothepin possesses excellent drug-like properties, with a particularly favorable metabolic stability (Hasanovic et al. 2018) (Table 1). However, methiothepin has a strong inhibition effect on the cardiac channel hERG harmful to its clinical development.

4.2 Astemizole

Astemizole is a second-generation H₁ antihistamine drug approved in 1986 for the treatment of allergic rhinitis and conjunctivitis. It has a high affinity for the histamine H₁ receptor, but also for the potassium channels Eag1 and hERG inducing serious adverse cardiac reactions. Accordingly, it was withdrawn from the market in 1999 for safety-related reasons (García-Quiroz et al. 2019). In this regard, the cryo-EM structure of hERG in complex with astemizole has been recently solved, showing the binding of astemizole to hERG (Asai et al. 2021). Several studies reported that when administrated in combination with a chemotherapeutic treatment, astemizole showed a significant correlation with reduced mortality among cancer patients. As an explanation, astemizole was suggested to sensitize cancer cells to chemotherapy and revert multidrug resistance (Ellegaard et al. 2016). Preclinical studies also suggested that astemizole could act synergistically in combination with chemotherapeutic agents. Indeed, astemizole was

shown to potentiate the cytotoxicity of dxr against dxr-resistant human leukemia cells (Ishikawa et al. 2000), and of gefitinib against human lung cancer (Chávez-López et al. 2017). This was attributed to an effect of astemizole on several proteins involved in cancer progression such as histamine receptors, ABC transporters and the potassium channels Eag1 and hERG (Jehle et al. 2011). However, the recent results obtained on hPtc1 expressing yeast suggest that this effect could also be due to the inhibition of the drug efflux activity of Ptc1 (Hasanovic et al. 2020). Indeed, this study revealed that astemizole inhibited the efflux of dxr but also that of cholesterol in hPtc1 expressing yeast. It also reported an increase of the cytotoxic, pro-apoptotic, anti-proliferative and anti-clonogenic effects of dxr on ACC cells when astemizole-dxr combo was used in which a non-cytotoxic concentration of dxr was applied. These results suggest that astemizole increased the sensitivity to dxr of yeast and ACC cells by inhibiting the dxr efflux activity of Ptc1 and that Ptc1 is a new target of astemizole.

4.3 Panicein A hydroquinone

Panicein A hydroquinone (PAH) is a meroterpenoids member of the panicein family produced by a marine sponge called *Haliclona* (*Soestella*) *mucosa*. This natural compound was shown to inhibit dxr efflux activity of Ptc1, and to increase the efficacy of dxr and cisplatin against melanoma cells *in vitro* (Fiorini et al. 2015). Due to the limited availability of natural PAH, its chemical synthesis was performed in order to further characterize its activity *in vitro* and *in vivo* (Signetti et al. 2020). The synthesized PAH proved to be as effective as the natural compound in increasing the cytotoxicity of dxr and inhibiting its efflux in melanoma cells. Experiments carried out in embryonic eggs showed that PAH was not toxic to the chicken embryos, and, when added in combination with dxr on melanoma cells xenografted on the eggs chorioallantoic membrane (CAM), it inhibited melanoma tumor growth more effectively than dxr alone. PAH was also shown to strongly increase the cytotoxicity of vemurafenib, even in resistant BRAF^{V600E} melanoma cells. The combination vemurafenib/PAH is synergistic, like the combinations of PAH with dxr or cisplatin. Moreover, wound-healing assays showed that addition of PAH to vemurafenib significantly reduced the reclosure of wounds compared to vemurafenib alone, suggesting that a PAH/vemurafenib combination could be more effective against the migration of BRAF^{V600E} melanoma cells than vemurafenib alone. As shown in Table 1, the metabolic stability of PAH is very low. The hydroxyquinone part of the PAH is rapidly oxidized by liver microsomes to give the quinone form which was shown to be inactive (Signetti et al. 2020). Therefore, PAH has been encapsulated in polylactic acid polymer nanoparticles to perform studies in mice. Encapsulated PAH (iP-PAH) proved to be very stable in the presence

of liver microsomes (more than 60 min) and well tolerated over three days to high doses (40 mg/kg) in acute treatment in mice (Signetti et al. 2020). The combination of iP-PAH and vemurafenib on melanoma xenografts in mice inhibited tumor growth more significantly than vemurafenib alone. This was accompanied by a decrease in proliferation and an increase in apoptosis of tumor cells, indicating that this combo is more cytotoxic against melanoma cells also *in vivo*. Moreover, metabolomics analysis showed that tumors from mice treated with the combo present higher amounts of vemurafenib in comparison with tumors from mice treated with vemurafenib alone confirming that the efficacy increase was due to Ptch1 drug efflux inhibition. Remarkably, these effects were achieved without obvious undesirable side effects for mice.

As for methiothepin, MicroScale Thermophoresis analyses suggested that PAH interacts specifically with Ptch1 in membranes prepared from hPtch1 yeast expressing, with a Kd of about 7 μ M.

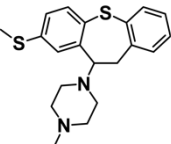
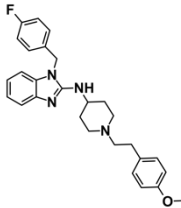
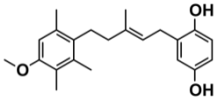
Inhibitor	Methiothepin		Astemizole		PAH		
Chemical structure							
LogD (pH 7.4)	3.5		2.9		5.2		
RLM stability, T _{1/2} (min)*	31		>60		1		
Cancer cell line	ACC	Melanoma Wild type	Melanoma BRAFV600E	ACC	Melanoma Wild type	Melanoma BRAFV600E	
In vitro PoC Chemotherapy	Doxorubicin	√ (6.6x)	√ (5.8x)	√ (15x)	√ (10x)	√ (128x)	√ (68x)
	Cisplatin	√	√ (3x)	√ (3.6x)	√	√	√
	Vemurafenib		√ (4x)	√ (10x)			√ (10x)
In vivo PoC Chemotherapy	Doxorubicin	√			√		
	Vemurafenib						√

Table 1. Profiling and activity of the Ptch1 drug efflux inhibitors methiothepin, astemizole and PAH. Profiling data were obtained experimentally (Hasanovich et al. 2018 and 2020, Signetti et al. 2020) except for the PAH LogD which was predicted using Stardrop (Optibrium, UK). √ indicates the combinations performed *in vitro*

and *in vivo*. The fold increase, induced by Ptch1 inhibitors, of *in vitro* cytotoxic effect of chemotherapeutic agents is indicated in brackets. **Metabolic stability in rat liver microsomes*

Profiling data and pharmacokinetics study indicate that methiothepin and astemizole possesses excellent drug-like properties, with a particularly favorable metabolic stability (Hasanovic et al. 2018 and 2020, Signetti et al. 2020) (Table 1). However, these molecules have a strong inhibition effect on the cardiac channel hERG harmful to their clinical development. PAH has less good drug properties but its low affinity for hERG and the opportunities for optimization make it an interesting hit.

The large body of data reviewed above, showing the role of Ptch1 in drug efflux, and its inhibition as a promising strategy for drug resistance overcome, led naturally to further efforts in understanding the mechanism of action and binding of the 3 hit inhibitors, in order to develop more potent compounds. In the following Section, we briefly review the outcome of structure- and ligand-based *in silico* studies on Ptch1 inhibition.

5. Structure- and ligand-based *in silico* studies on Ptch1 inhibition

Computer-aided drug discovery is a particularly attractive alternative to expensive high throughput screenings and other experimental methods in the early stages of ligand discovery. With the aim of increasing the efficiency of *in-silico* drug design, several protocols combining different computational techniques have been developed: docking (Forli 2015, Amaro et al. 2018), structure-prediction approaches (Jumper et al. 2021, Tunyasuvunakool et al. 2021), molecular dynamics simulations (see e.g., the reviews by De Vivo et al. 2016, Hollingsworth and Dror 2018, and Salo-Ahen et al. 2021, and references therein), machine/deep learning methods (Raschka and Kaufman 2020) are few examples. These efforts aim to improve the description of both receptors and ligands accounting for structural and dynamical features, often barely observable in experiments, by keeping reasonable computational costs. Although characterized by an impressive reliability, computational protocols present still several steps relying on experimental (especially structural) data. Thus, the description of the main outcomes coming from computational studies on Ptch1 will be preceded by an overview of the available structural data.

5.1 Structural data in support of Ptch1 transport activity

Several cryo-EM structures of Ptch1, both in its monomeric and dimeric form, in complex with or without its ligand Sonic Hedgehog (Shh) have been solved recently (Gong et

al. 2018; Qi et al. 2018; Zhang et al. 2018; Qian et al. 2019; Qi et al. 2019; Rudolf et al. 2019) (Fig. 4). Besides unveiling the details about the Ptch1-Shh recognition and interaction, the structural data gave mechanistic insights on the role of Ptch1 in sterol transport. Several sterol-like densities were observed in the cryo-EM maps of Ptch1, in agreement with the hypothesis as sterol transporter (Fig. 4B). In all structures both free and bound to the Shh C terminal domain, sterol-like densities were found in the SSD, a V shaped cavity formed between helices TM2, TM3 and TM4 (site 1) (and in the symmetry-related helices TM8, TM9, and TM10) and in the extracellular domain (ECD)1 (site 2) (Fig. 4A). The SSD is located in the transmembrane domain (TMD) (Fig. 4B site 1) which shares the same 12 helices fold as other RND homologs, such as AcrB from *Escherichia coli*, HpnN from *Burkholderia multivorans* and the eukaryotic transporters NPC1 and NPC1L1. For instance, in the case of NPC1, which is responsible for lysosomal sterol trafficking, the SSD domain represents the exit point for sterols leading to their accumulation into the lysosomes. Cholesterol binding site 2 has been found to bind both free cholesterol and cholesterolated C-terminus of Shh (Rudolf et al. 2019) (Fig. 4B site 2), and indeed from a structural point of view this pocket looks uniquely adapted to cholesterol and Shh binding being lined with aromatic and aliphatic side chains. An additional sterol-like density was observed located between ECD1, ECD2 and above the TMD, a highly dynamic area of the receptor mainly delimited by loops (site 3) (Fig. 4C).

Unfortunately, the resolution of the cryo-EM maps (3.5 Å at best) does not allow to precisely identify the ligands and their binding mode to Ptch1. However, according to the transport activity of the protein, a hydrophobic conduit has been proposed to extend from the ECD to two openings, both in the TMD of the protein, namely above the SSD and the symmetry-related segment (Fig. 4A). Direct cholesterol quantification measurements showed that Ptch1 reduces the inner plasma membrane cholesterol concentration in a manner dependent on the integrity of this putative conduit (Zhang et al. 2018). All together these elements support the generally accepted hypothesis that Hh signaling and Smo regulation depend on the cholesterol distribution in the plasma membrane, which is itself regulated by Ptch1. In this scenario, Ptch1 sterol transport occurs together with a conformational switching that harnesses energy from protons flowing down an electrochemical gradient. Like for the well-studied prokaryotic RND transporters, a protonation-deprotonation of a charged triad, namely D₅₁₃D₅₁₄E₁₀₉₅ located on TM4 and TM10, drives the whole process of conformational change. Moreover, the efflux of chemotherapeutics mediated by Ptch1 and related to MDR has been proposed to occur in cancer cells according to the same “proton motive force” mechanism and through the cholesterol transport conduit. Unfortunately, no structure of Ptch1 in complex with

a chemotherapeutic agent or efflux inhibitors is available yet. Whether the inhibitors of Ptch1 drug efflux compete themselves with the transport mechanism by being transported by Ptch1 or binding to a specific pocket located along the cholesterol conduit remains to be elucidated.

5.2 Inhibitor binding site identification and analysis

The intrinsic nature of the transporter Ptch1 suggests that it adopts different conformations during its functioning, thus making difficult to precisely identify the binding site or the mechanism of action of its inhibitors. However, the most plausible region for the binding of inhibitors seems to be the cavity between ECD1 and ECD2 right above the TMD (site 3), called central cavity hereafter. Several experimental findings support this hypothesis: (a) this pocket is formed along the hydrophobic conduit and cholesterol is found to bind inside it (Zhang et al. 2018); (b) being large enough and lined by chemically different residues, this cavity is suitable to be occupied by chemically different ligands, furthermore it is constructed between loops which suggests high flexibility and ability to adapt to compounds differing in shape and size (Fig. 4C); (c) eight of the central cavity residues, namely L128, T499, D776, Y1013, W1018, Q1020, V1081, F1152, are responsible for diseases when mutated (Dingerdissen et al. 2018) (Fig. 4C), and many of them are conserved among the Patched family of proteins (Hasanovic et al. 2020) suggesting their importance in the transport activity of the protein; (d) in the structurally related NPC1 and NPC1L1, cholesterol transport inhibitors, itraconazole and ezetimibe respectively, bind in the related cavity (Long et al. 2020; Hu et al. 2021) (Fig. 4D-E).

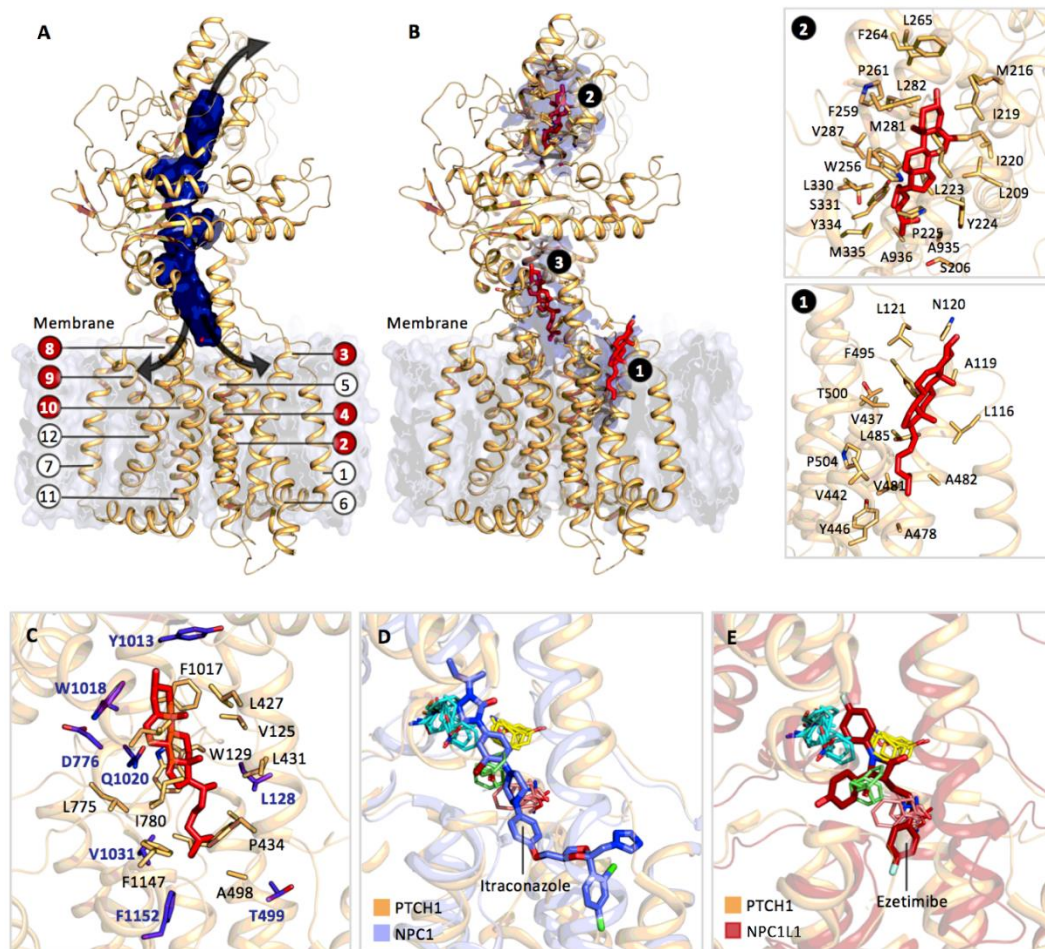


Figure 4. Overall structure of Ptcp1 (PDB ID 6N7H, chain A) (cholesterol is shown in red stick representation). A) The hydrophobic conduit proposed for cholesterol translocation is represented in blue surface: it extends from the ECD1 to two openings in the TMD, one exit is located in the SSD (helices composing SSD are highlighted in red) and the other in the symmetry related helices TM8, TM9 and TM10 (highlighted in red); B) The 3 binding sites for cholesterol are highlighted: site 1 in the SSD, site 2 in the ECD1 and site 3 in the core of the transporter in a highly dynamic region. The residues lining binding sites 1 and 2 (5Å from the ligand) are shown in light orange stick representation; C) Site 3 or central cavity: the residues lining the binding site 3 (5Å from the ligand) are shown in light orange stick representation and the residues responsible for damaged phenotype when mutated are highlighted in purple. D) Superimposition between Ptcp1 (PDB ID 6N7H, chain A, represented in light orange cartoon) and NPC1 (PDB ID 6UOX, represented in light blue cartoon) in complex with its inhibitor itraconazole. E) Superimposition between Ptcp1 (PDB ID 6N7H, monomer A, represented in light orange cartoon) and NPC1L1 (PDB ID 7DFZ, represented in light firebrick cartoon) in complex with its inhibitor ezetimibe. In panel D(E) chemical probes identifying hot spots on Ptcp1 surface are mainly located in the same region in which itraconazole (ezetimibe) binds to NPC1 (NPC1L1).

5.3 *In silico* studies of Ptcp1

Prediction and identification of inhibitors of multidrug efflux transporters is an active area of research. Many *in silico* studies have been published over the years, addressing mechanisms of recognition and binding of different compounds by a large variety of systems ranging from human ABC transporters (e.g., Tangella et al. 2021) to bacterial proteins of the RND family

(e.g., Atzori et al. 2019). Concerning Ptch1, computational investigations were focused on cholesterol transport (Rudolf et al. 2019), recognition and binding (Kovachka et al. 2021), and mechanism of drug efflux and of inhibition (Hasanovic et al. 2020; Durand et al. 2021; Signetti et al. 2020). Extensive molecular dynamics simulations of cholesterol molecules interacting with the transporter complemented available structural data by demonstrating cholesterol transport (Rudolf et al. 2019).

More recent *in silico* investigation supported experimental data by further highlighting the prominent role of site 3 in Ptch1 ligand binding (Kovachka et al. 2021). More specifically, a pocket detection analysis (performed on the PDB ID 6N7H, chain A) identified the central cavity as the largest cavity present on Ptch1. In addition, a fragment-based binding site search campaign, conducted with the primary goal to identify protein regions able to simultaneously bind to chemically different probes, revealed "hot spots" mainly located in the central cavity. Interestingly, when superimposing the structure of Ptch1 and NPC1 or NPC1L1 in complex respectively with itraconazole or ezetimibe (PDB IDs of NPC1 and NPC1L1: 6UOX and 7DFZ) with the hot spot map of Ptch1 reported in (Kovachka et al. 2021), the ligand from the former covers very well the predicted hot spots of the latter (Fig. 4C-E). However other weaker hot spots were found along the sterol channel including the ECD1 pocket.

Regarding the inhibition mechanism, the first structural insights on the binding of astemizole, methiothepin and PAH to Ptch1 were also revealed by molecular docking studies (Hasanovic et al. 2020; Durand et al. 2021; Signetti et al. 2020). In all the docking protocols used, only one conformation of Ptch1 was used and flexibility was allowed only for the ligand while the protein was kept rigid. A monomeric structure of Ptch1 with three natively present binding pockets was chosen (Qian et al. 2019). It is worth to note that due to the high protein flexibility, other cavities might play a role in the transport mechanism. The predicted binding modes of the three inhibitors in the central cavity of Ptch1 are shown in Figure 5. The superimposition of the docking poses reveals a remarkably similar binding mode for astemizole and methiothepin. For instance, the lipophilic dihydrodibenzothiepine moiety of methiothepin superimposes well to the (4-fluorobenzyl)benzimidazol moiety of astemizole and the two are in contact with the same residues in the upper part of the pocket, namely I791, F795, Y801, Y1013 (highlighted in blue bold in Table 2) and F1017. Likewise, the piperazinyl and piperidinyl moiety of methiothepin and astemizole respectively, both positively charged at physiological pH of 7.4 are oriented towards the same residues. On the other hand, while methiothepin's methyl group seems not to be involved in any specific interaction, astemizole's lipophilic tail is buried towards the TMD of Ptch1 with the terminal phenyl ring being involved in π - π interactions with

the aromatic residues W129 and F434. This lipophilic tail is what astemizole and PAH share, both from structural and binding mode point of view. PAH terminal phenyl ring and flexible pentene link well superimpose to astemizole's tail and piperazinyl cycle establishing the same π - π interactions with the aromatic residues W129 and F434 and lipophilic patches with A498, A569 and L570. In addition to the π - π and lipophilic interactions that PAH shares with astemizole, the hydroquinone moiety of the ligand is involved in H-bond with the backbone of L775. Interestingly, *in silico* docking analyses revealed that doxorubicin and vemurafenib, two drugs shown to be transported out of cancer cells by Ptch1, were able to bind in the central cavity (Signetti et al. 2020). One can observe at least one hydrogen bond with nearby amino acids for doxorubicin and vemurafenib (L775 or D776), both with the oxygen of the peptide bond. The structural diversity between methiothepin and PAH does not allow a straight comparison of their binding modes except for similar interactions with lipophilic residues lining the central part of the pocket (highlighted in black bold in Table 2).

A more recent computational study reporting binding site identification and bioactive ligand conformation assessment aimed at discriminating between good and poor binders for Ptch1 (Kovachka et al. 2021). In this work, all compounds were blindly docked to the monomeric structure of Ptch1, and ligand flexibility was implicitly considered by employing conformations extracted from all-atom μ s-long MD simulations of ligands in water solution. This ensemble docking strategy enabled to obtain a statistical contact analysis emphasizing the importance of prevalent protein residues, rather than focusing on specific binding modes. Besides the identification of the central cavity (site 3) as the putative binding site of PAH, one of the main outcomes of the study was to discover that predicted binding affinities are better for open and elongated conformations of the ligands than for closed and spherical (compact) conformations. Since the active compounds were mostly found in an open conformation during the MD simulation, this led to the interesting general conclusion that when the latter is prevalent in water solution the corresponding compound is most likely going to be a good Ptch1 efflux inhibitor.

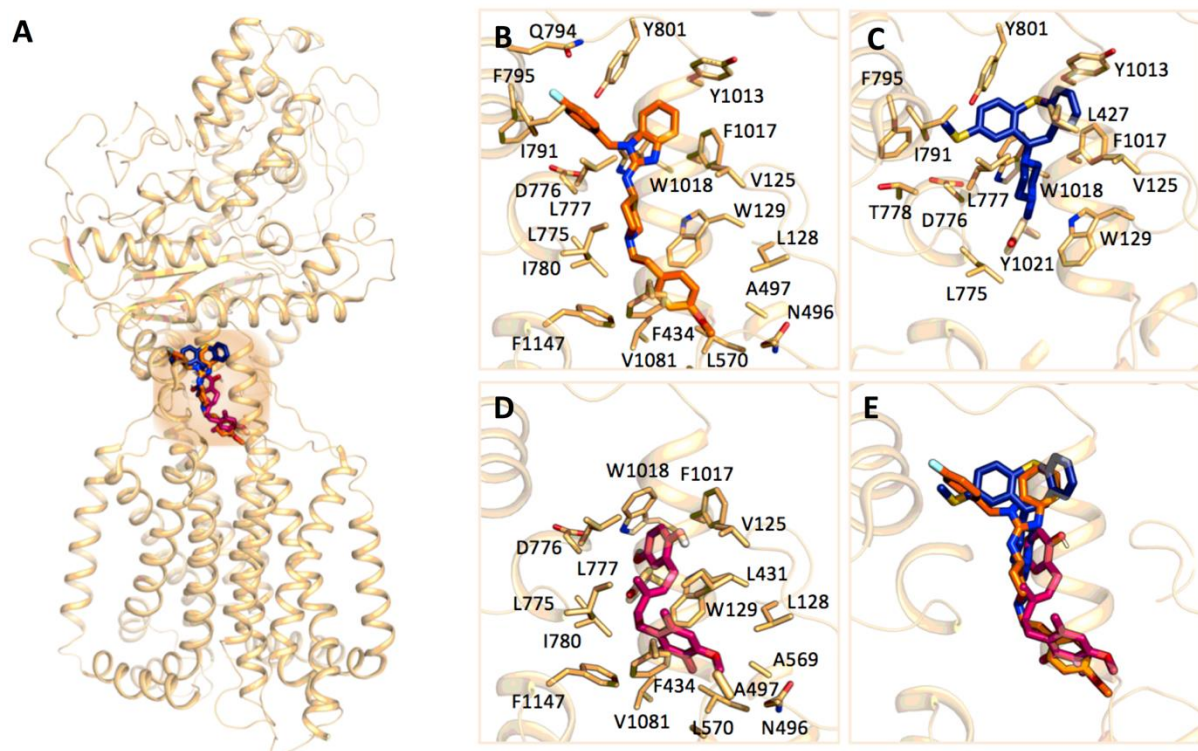


Figure 5. Predicted binding modes of the known inhibitors in the central cavity of Ptch1. A) Astemizole, methiothepin and PAH bound to the central cavity (site 3) of Ptch1, residues within 5 Å of the ligand are shown in light orange sticks. Best docking poses of astemizole, methiothepin, and PAH are reported in panels B), C), and D) respectively; E) Superimposition of the three inhibitors inside the binding site 3 (astemizole, methiothepin and PAH in orange, blue and magenta respectively): the lipophilic dihydrodibenzothiepine moiety of methiothepin superimposes well to the lipophilic part of astemizole, thus sharing contacts with the same residues of Ptch1. The piperazinyl and piperidinyli moiety of methiothepin and astemizole, respectively, both positively charged at physiological pH of 7.4, are oriented towards the same residues. The lipophilic tale of astemizole and PAH are buried towards the TMD of Ptch1.

Ligand	Residues within 5Å distance from ligand
Astemizole	V125, L128, W129, F434, N496, A497, A569, L570, L775, D776, L777, I780, I791, Q794, F795, Y801, Y1013, F1017, W1018, V1081, F1147.
Methiothepin	V125, W129, L427, L775, D776, L777, T778, I791, F795, Y801, Y1013, F1017, W1018, Y1021.
PAH	V125, L128, W129, L431, F434, N496, A497, A498, A569, L570, G774, L775, D776, L777, I780, F1017, W1018, V1081, F1147.

Table 2. Residues surrounding the binding poses of the three inhibitors at 5 Å distance. Residues common to all compounds are highlighted in black bold, the common residues found for astemizole and methiothepin are highlighted in blue bold, and the common residues for astemizole and PAH are highlighted in red bold.

6 Towards the design of a next generation of inhibitors

Despite promising results demonstrating the efficacy of Ptch1 drug efflux inhibition, the design of new more potent compounds is necessary. A comparative analysis that could help to build a pharmacophore model useful for the design and synthesis of the next generation of inhibitors can be valuable to this aim. Even though astemizole, methiothepin and PAH have a very different chemical structure (for instance PAH does not have any ionizable group while methiothepin and astemizole are both positively charged at physiological pH), one can speculate that these compounds are all able to bind to Ptch1 and inhibit its efflux activity by means of the same mechanism of action.

Some "standard" molecular descriptors of these inhibitors are comparatively listed in Table 3. In addition to the reported "standard" descriptors, associated with a single, static configuration of the molecules, it is instructive to compare their dynamical properties to learn more about the bioactive conformation of the "ideal" inhibitor. Following the investigation on PAH and derivatives (Kovachka et al. 2021), we here applied the same all-atom 1 μ s-long MD simulations protocol for astemizole and methiothepin (see Kovachka et al. 2021 for further details). Both molecules have been simulated with a net positive charge on the piperazinyl and piperidinyl moiety respectively (according to pKa values and ionization state at pH 7.4). The resulting comparison is reported in Figure 6. Given the poor degree of freedom for methiothepin, the corresponding RMSD and RMSF graphs show a relatively low divergence from the average structure with only two main conformations that are very similar (RMSD 1.84 Å) and account for more than 95% of the total simulation time. On the other hand, as previously reported (Kovachka et al. 2021), PAH is the most flexible ligand and thus it assumes many different conformations during the simulation (highest RMSD value observed for this compound). Two main states can however be observed for this ligand, an open (cylindric) and a closed one (spherical), where the aromatic rings are establishing intramolecular π - π interactions, with the open conformation being prevalently adopted (XX vs. YY of the total simulation time). Astemizole has an intermediate behavior, being the compound balanced between rigid and rotatable bonds. As can be appreciated from the RMSF graph, the highest fluctuation is given by the lipophilic tail and the fluorophenyl arm while the rest of the molecule has a relatively stable conformation.

	Astemizole	Methiothepin	PAH
Chemical Formula	C ₂₈ H ₃₁ FN ₄ O	C ₂₀ H ₂₀ N ₂ S ₂	C ₂₂ H ₂₈ O ₃
Molecular Weight	458.58	356.55	340.46
Atoms; Heavy atoms	65; 34	48; 24	53; 25

Rotatable Bonds	8	2	13
H bonds donors/acceptors*	1 / 5	0 / 2	2 / 3
LogP	5.6	4.7	6.5
Van der Waals Volume (A ³)	427.81	330.94	343.35
Molecular Surface Area (A ²)	698.06	516.45	563.44
Polar Surface Area (A ²)**	42.52	7.68	49.69
pKa	8.73; 6.24	7.8; 2.01	9.53; 11.42

Table 3. Comparison between some molecular descriptors of the three known Ptch1 inhibitors as computed with the Marvin ChemAxon suite of programs (Marvin 17.21.0, ChemAxon, <https://chemaxon.com>). *The molecule is considered neutral; **the major microspecies at pH 7.40 is considered.

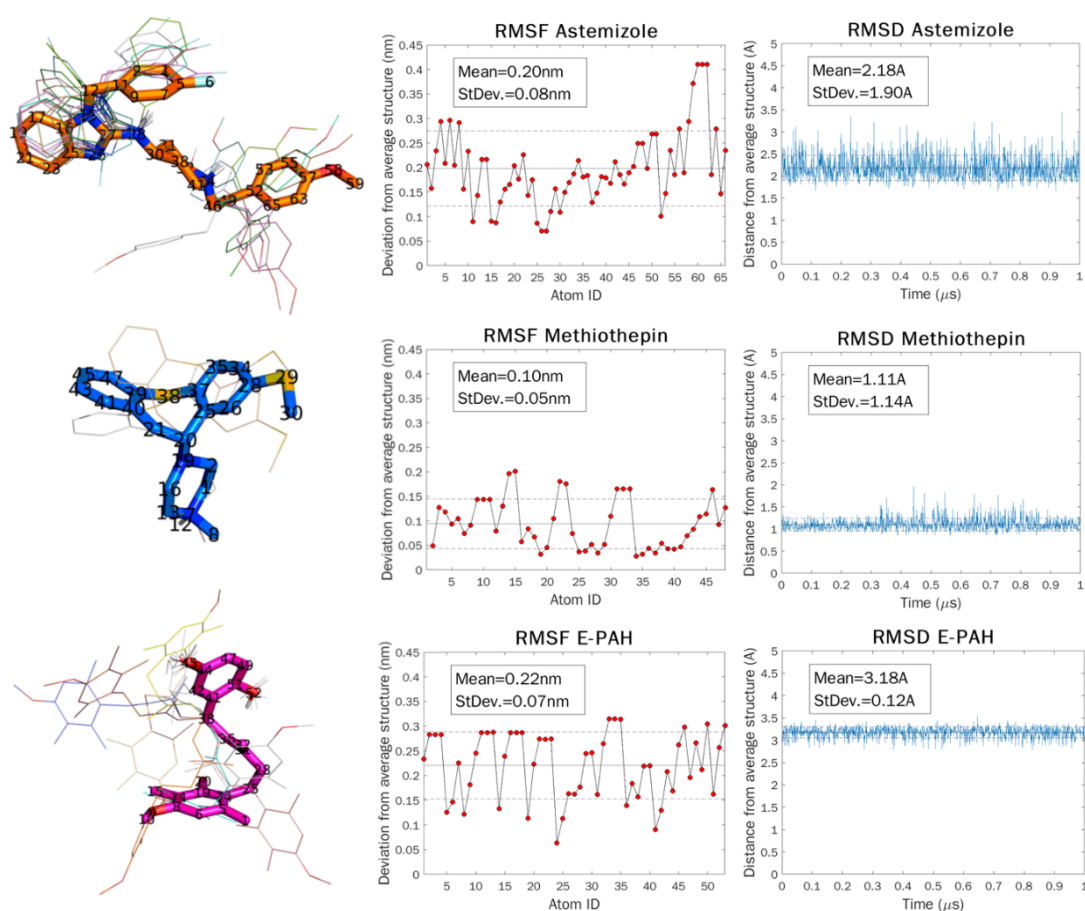


Figure 6. Conformational analysis of astemizole (1st line), methiothepin (2nd line) and E-PAH (3rd line). The average structures of the trajectory are represented in thick stick while the cluster representatives are represented in lines (10 cluster representatives for astemizole and PAH, 2 cluster representatives for methiothepin). For easier interpretation of the RMSF graph, the atom IDs of the heavy atoms for each molecule are shown in black in the stick representation.

To go deeper into the comparison between the known inhibitors of Ptch1, we here performed a 3D structural ligand alignment using the Flexi-LS-align module of the webserver LS-align (Hu et al. 2018). We chose methiothepin and astemizole as the first alignment pair.

Given the rigid structure of methiothepin, we chose to use as ligand template the average conformation taken from the MD simulation, while astemizole was allowed flexible. Fifteen atoms out of 19 were aligned with $\text{RMSD} < 1\text{\AA}$, we found significant overlap between the dihydrodibenzothiepine and the (4-fluorobenzyl)benzimidazol moiety of methiothepin and astemizole, respectively, while the piperazinyl and piperidinyl moiety were quite well aligned (Fig. 7A). The lipophilic 4-(methoxyphenyl)ethyl tail of astemizole did not take part of the alignment so we were not able to assess its 3D orientation. Since there are some structural similarities between PAH and astemizole, such as the hydrophobic tail and the presence of a linker connecting two aromatic portions, we next performed an alignment between these 2 molecules. We observed a good overlap between the methoxyphenyl portions of the 2 molecules in almost all the alignment pairs and the pentene linker or PAH overlaps with the piperazinyl linker of astemizole (Fig. 7B). On the other hand, there was no significant overlap between the hydroquinone and the (4-fluorobenzyl)benzimidazol, due to both the shorter length of PAH linker and the chemical difference in terms of H bond donors/acceptors.

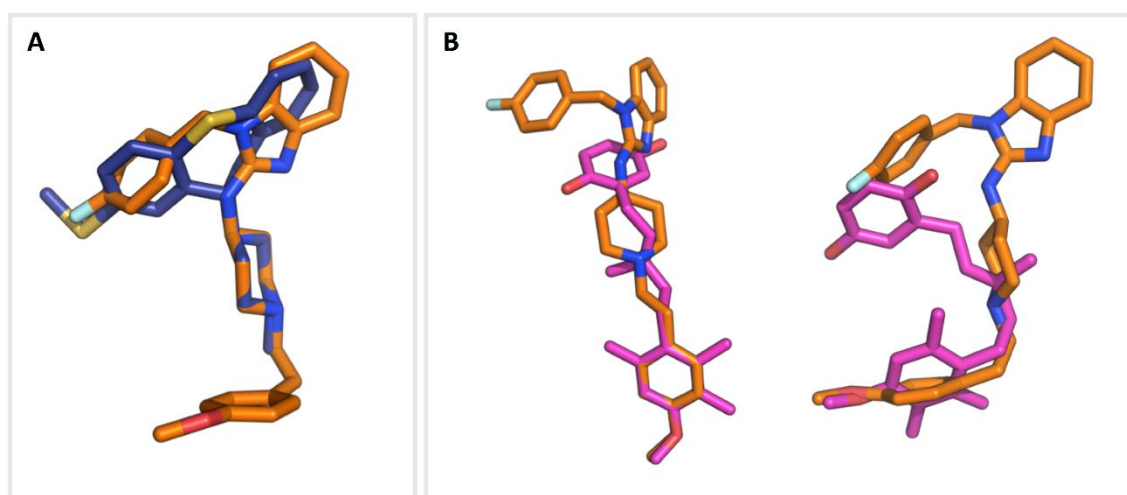


Figure 7. Structural comparison between the known inhibitors of Ptch1. A) Structural Alignment of astemizole and methiothepin represented in orange and blue respectively. B) Structural Alignment of astemizole and PAH represented in orange and magenta respectively.

Based on the above results, we speculate that PAH binds to Ptch1 in a slightly different way than astemizole and methiothepin, and this is possible due to the high flexibility of the central cavity and its ability to adapt as previously described. Complementary to this ligand-based approach, MD-based simulations would represent a natural follow-up of protein-ligand molecular docking studies reviewed above. Evaluation of pose stability, coupled with estimates of the energetics of binding, and quantitative assessment of the per-residue contribution to the ligand-receptor interactions are all important information that would lead to the design of new

inhibitors. Studies adopting this protocol and successfully addressing inhibition of RND transporters have been published over the last years (Sjuts et al. 2016, Reading et al. 2020).

Declaration of competing interest

The authors declare that they have no known competing financial interests or personal relationships that could have appeared to influence the work reported in this paper.

Acknowledgements

This research has received funding from the French government through the UCAJEDI Investments in the Future project with the reference number ANR-15-IDEX-01, Region PACA and BoostUrCareer project European Union's Horizon 2020 research and innovation program under grant agreement no. 847581. G.M. and P. R. acknowledge support by National Institute of Allergy and Infectious Diseases/NIH grant no. R01AI136799.

References

- [1] N. Ahalawat, J. Mondal, An Appraisal of Computer Simulation Approaches in Elucidating Biomolecular Recognition Pathways, *J. Phys. Chem. Lett.* 12 (2021) 633–641. <https://doi.org/10.1021/acs.jpcclett.0c02785>.
- [2] R.E. Amaro, J. Baudry, J. Chodera, Ö. Demir, J.A. McCammon, Y. Miao, J.C. Smith, Ensemble Docking in Drug Discovery, *Biophys. J.* 114 (2018) 2271–2278. <https://doi.org/10.1016/j.bpj.2018.02.038>.
- [3] T. Asai, N. Adachi, T. Moriya, H. Oki, T. Maru, M. Kawasaki, K. Suzuki, S. Chen, R. Ishii, K. Yonemori, S. Igaki, S. Yasuda, S. Ogasawara, T. Senda, T. Murata, Cryo-EM Structure of K⁺-Bound hERG Channel Complexed with the Blocker Astemizole, *Structure.* 29 (2021) 203–212.e4. <https://doi.org/10.1016/j.str.2020.12.007>.
- [4] M. Aszterbaum, A. Rothman, R.L. Johnson, M. Fisher, J. Xie, J.M. Bonifas, X. Zhang, M.P. Scott, J. Epstein, Identification of mutations in the human PATCHED gene in sporadic basal cell carcinomas and in patients with the basal cell nevus syndrome, *J. Invest. Dermatol.* 110 (1998) 885–888. <https://doi.org/10.1046/j.1523-1747.1998.00222.x>.
- [5] A. Atzori, G. Mallocci, J.D. Prajapati, A. Basciu, A. Bosin, U. Kleinekathöfer, J. Dreier, A. V. Vargiu, P. Ruggerone, Molecular Interactions of Cephalosporins with the Deep Binding Pocket of the RND Transporter AcrB, *J. Phys. Chem. B.* 123 (2019) 4625–4635. <https://doi.org/10.1021/acs.jpcc.9b01351>.
- [6] A. Balzerano, E. Paccosi, L. Proietti-De-Santis, Evolutionary Mechanisms of Cancer Suggest Rational Therapeutic Approaches, *Cytogenet. Genome Res.* 161 (2021) 362–371.

<https://doi.org/10.1159/000516530>.

- [7] M. Bidet, O. Joubert, B. Lacombe, M. Ciantar, R. Nehmé, P. Mollat, L. Brétilon, H. Faure, R. Bittman, M. Ruat, I. Mus-Veteau, The hedgehog receptor patched is involved in cholesterol transport, *PLoS One*. 6 (2011) 1–11. <https://doi.org/10.1371/journal.pone.0023834>.
- [8] M. Bidet, A. Tomico, P. Martin, H. Guizouarn, P. Mollat, I. Mus-Veteau, The Hedgehog receptor patched functions in multidrug transport and chemotherapy resistance, *Mol. Cancer Res.* (2012). <https://doi.org/10.1158/1541-7786.MCR-11-0578>.
- [9] B.R. Brooks, C.L. Brooks, A.D. Mackerell, L. Nilsson, R.J. Petrella, B. Roux, Y. Won, G. Archontis, C. Bartels, S. Boresch, A. Caflisch, L. Caves, Q. Cui, A.R. Dinner, M. Feig, S. Fischer, J. Gao, M. Hodoscek, W. Im, K. Kuczera, T. Lazaridis, J. Ma, V. Ovchinnikov, E. Paci, R.W. Pastor, C.B. Post, J.Z. Pu, M. Schaefer, B. Tidor, R.M. Venable, H.L. Woodcock, X. Wu, W. Yang, D.M. York, M. Karplus, CHARMM: The biomolecular simulation program, *J. Comput. Chem.* 30 (2009) 1545–1614. <https://doi.org/10.1002/jcc.21287>.
- [10] K. Bukowski, M. Kciuk, R. Kontek, Mechanisms of multidrug resistance in cancer chemotherapy1. Bukowski K, Kciuk M, Kontek R. Mechanisms of multidrug resistance in cancer chemotherapy. *Int J Mol Sci.* 2020;21(9). doi:10.3390/ijms21093233, *Int. J. Mol. Sci.* 21 (2020).
- [11] P. Carloni, U. Rothlisberger, M. Parrinello, The role and perspective of ab initio molecular dynamics in the study of biological systems, *Acc. Chem. Res.* 35 (2002) 455–464. <https://doi.org/10.1021/ar010018u>.
- [12] D.A. Case, T.E. Cheatham, T. Darden, H. Gohlke, R. Luo, K.M. Merz, A. Onufriev, C. Simmerling, B. Wang, R.J. Woods, The Amber biomolecular simulation programs, *J. Comput. Chem.* 26 (2005) 1668–1688. <https://doi.org/10.1002/jcc.20290>.
- [13] M. de G. Chávez-López, V. Zúñiga-García, E. Hernández-Gallegos, E. Vera, C.A. Chasiquiza-Anchatuña, M. Viteri-Yáñez, J. Sanchez-Ramos, E. Garrido, J. Camacho, The combination astemizole–gefitinib as a potential therapy for human lung cancer, *Oncotargets Ther.* 10 (2017) 5795–5803. <https://doi.org/10.2147/OTT.S144506>.
- [14] Y.C. Chen, Beware of docking!, *Trends Pharmacol. Sci.* 36 (2015) 78–95. <https://doi.org/10.1016/j.tips.2014.12.001>.
- [15] A. Chidambaram, A.M. Goldstein, M.R. Gailani, B. Gerrard, S.J. Bale, J.J. DiGiovanna, A.E. Bale, M. Dean, Mutations in the human homologue of the *Drosophila* patched gene in Caucasian and African-American nevoid basal cell carcinoma syndrome patients, *Cancer Res.* 56 (1996) 4599–4601.
- [16] C.R. Cochrane, A. Szczepny, D.N. Watkins, J.E. Cain, Hedgehog signaling in the maintenance of cancer stem cells, *Cancers (Basel)*. (2015). <https://doi.org/10.3390/cancers7030851>.
- [17] I.A. Cree, P. Charlton, Molecular chess? Hallmarks of anti-cancer drug resistance, *BMC Cancer.* 17 (2017) 1–8. <https://doi.org/10.1186/s12885-016-2999-1>.
- [18] M. Damaghi, J.W. Wojtkowiak, R.J. Gillies, pH sensing and regulation in cancer, *Front. Physiol.* (2013). <https://doi.org/10.3389/fphys.2013.00370>.
- [19] M. De Vivo, M. Masetti, G. Bottegoni, A. Cavalli, Role of Molecular Dynamics and Related

- Methods in Drug Discovery, *J. Med. Chem.* 59 (2016) 4035–4061. <https://doi.org/10.1021/acs.jmedchem.5b01684>.
- [20] H.M. Dingerdissen, J. Torcivia-Rodriguez, Y. Hu, T.C. Chang, R. Mazumder, R. Kahsay, BioMuta and BioXpress: Mutation and expression knowledgebases for cancer biomarker discovery, *Nucleic Acids Res.* 46 (2018) D1128–D1136. <https://doi.org/10.1093/nar/gkx907>.
- [21] N. Durand, M. Simsir, L. Signetti, F. Labbal, R. Ballotti, I. Mus-Veteau, Methiothepin increases chemotherapy efficacy against resistant melanoma cells, *Molecules.* 26 (2021). <https://doi.org/10.3390/molecules26071867>.
- [22] J. Eberhardt, D. Santos-Martins, A.F. Tillack, S. Forli, AutoDock Vina 1.2.0: New Docking Methods, Expanded Force Field, and Python Bindings, *J. Chem. Inf. Model.* 61 (2021) 3891–3898. <https://doi.org/10.1021/acs.jcim.1c00203>.
- [23] A.M. Ellegaard, C. Dehlendorff, A.C. Vind, A. Anand, L. Cederkvist, N.H.T. Petersen, J. Nylandsted, J. Stenvang, A. Mellemgaard, K. Østerlind, S. Friis, M. Jäättelä, Repurposing Cationic Amphiphilic Antihistamines for Cancer Treatment, *EBioMedicine.* 9 (2016) 130–139. <https://doi.org/10.1016/j.ebiom.2016.06.013>.
- [24] L. Fiorini, I. Mus-Veteau, Method to Screen Multidrug Transport Inhibitors Using Yeast Overexpressing a Human MDR Transporter, in: *Methods Protoc.*, 2016: pp. 303–318. https://doi.org/10.1007/978-1-4939-3637-3_19.
- [25] L. Fiorini, M.A. Tribalat, L. Sauvard, J. Cazareth, E. Lalli, I. Broutin, O.P. Thomas, I. Mus-Veteau, Natural paniceins from mediterranean sponge inhibit the multidrug resistance activity of Patched and increase chemotherapy efficiency on melanoma cells, *Oncotarget.* (2015). <https://doi.org/10.18632/oncotarget.4162>.
- [26] S. Forli, A.J. Olson, A force field with discrete displaceable waters and desolvation entropy for hydrated ligand docking, *J. Med. Chem.* 55 (2012) 623–638. <https://doi.org/10.1021/jm2005145>.
- [27] S. Forli, Charting a path to success in virtual screening, *Molecules.* 20 (2015) 18732–18758. <https://doi.org/10.3390/molecules201018732>.
- [28] R.A. Friesner, J.L. Banks, R.B. Murphy, T.A. Halgren, J.J. Klicic, D.T. Mainz, M.P. Repasky, E.H. Knoll, M. Shelley, J.K. Perry, D.E. Shaw, P. Francis, P.S. Shenkin, Glide: A New Approach for Rapid, Accurate Docking and Scoring. 1. Method and Assessment of Docking Accuracy, *J. Med. Chem.* 47 (2004) 1739–1749. <https://doi.org/10.1021/jm0306430>.
- [29] T. Gambichler, M. Dreißigacker, D. Kasakovski, M. Skrygan, U. Wieland, S. Silling, J. Gravemeyer, A. Melior, A. Cherouny, M. Stücker, E. Stockfleth, M. Sand, J.C. Becker, Patched 1 expression in Merkel cell carcinoma, *J. Dermatol.* 48 (2021) 64–74. <https://doi.org/10.1111/1346-8138.15611>.
- [30] J. García-Quiroz, M.E. González-Gonzalez, L. Díaz, D. Ordaz-Rosado, M. Segovia-Mendoza, H. Prado-García, F. Larrea, R.G. Becerra, Astemizole, an Inhibitor of Ether-A-Go-Go-1 Potassium Channel, Increases the Activity of the Tyrosine Kinase Inhibitor Gefitinib in Breast Cancer Cells, *Rev. Investig. Clin.* 71 (2019) 186–194. <https://doi.org/10.24875/RIC.18002840>.
- [31] E. Giroux-Leprieur, A. Costantini, V.W. Ding, B. He, Hedgehog signaling in lung cancer: From oncogenesis to cancer treatment resistance, *Int. J. Mol. Sci.* 19 (2018) 1–17.

<https://doi.org/10.3390/ijms19092835>.

- [32] X. Gong, H. Qian, P. Cao, X. Zhao, Q. Zhou, J. Lei, N. Yan, Structural basis for the recognition of Sonic Hedgehog by human Patched1, *Science* (80-.). 361 (2018). <https://doi.org/10.1126/science.aas8935>.
- [33] A. Gonniissen, S. Isebaert, C. Perneel, C.M. McKee, F. Van Utterbeeck, E. Lerut, C. Verrill, R.J. Bryant, S. Joniau, R.J. Muschel, K. Haustermans, Patched 1 Expression Correlates with Biochemical Relapse in High-Risk Prostate Cancer Patients, *Am. J. Pathol.* 188 (2018) 795–804. <https://doi.org/10.1016/j.ajpath.2017.11.019>.
- [34] I.A. Guedes, C.S. de Magalhães, L.E. Dardenne, Receptor-ligand molecular docking, *Biophys. Rev.* 6 (2014) 75–87. <https://doi.org/10.1007/s12551-013-0130-2>.
- [35] H. Hahn, C. Wicking, P.G. Zaphiropoulos, M.R. Gailani, S. Shanley, A. Chidambaram, I. Vorechovsky, E. Holmberg, A.B. Unden, S. Gillies, K. Negus, I. Smyth, C. Pressman, D.J. Leffell, B. Gerrard, A.M. Goldstein, M. Dean, R. Toftgard, G. Chenevix-Trench, B. Wainwright, A.E. Bale, Mutations of the human homolog of drosophila patched in the nevoid basal cell carcinoma syndrome, *Cell.* 85 (1996) 841–851. [https://doi.org/10.1016/S0092-8674\(00\)81268-4](https://doi.org/10.1016/S0092-8674(00)81268-4).
- [36] T.A. Halgren, R.B. Murphy, R.A. Friesner, H.S. Beard, L.L. Frye, W.T. Pollard, J.L. Banks, Glide: A New Approach for Rapid, Accurate Docking and Scoring. 2. Enrichment Factors in Database Screening, *J. Med. Chem.* 47 (2004) 1750–1759. <https://doi.org/10.1021/jm030644s>.
- [37] D. Hamelberg, J. Mongan, J.A. McCammon, Accelerated molecular dynamics: A promising and efficient simulation method for biomolecules, *J. Chem. Phys.* 120 (2004) 11919–11929. <https://doi.org/10.1063/1.1755656>.
- [38] T.J. Harpole, L. Delemotte, Conformational landscapes of membrane proteins delineated by enhanced sampling molecular dynamics simulations, *Biochim. Biophys. Acta - Biomembr.* 1860 (2018) 909–926. <https://doi.org/10.1016/j.bbamem.2017.10.033>.
- [39] A. Hasanovic, I. Mus-Veteau, Targeting the Multidrug Transporter Ptch1 Potentiates Chemotherapy Efficiency, *Cells.* 7 (2018) 107. <https://doi.org/10.3390/cells7080107>.
- [40] A. Hasanovic, C. Ruggiero, S. Jung, I. Rapa, L. Signetti, M. Ben Hadj, M. Terzolo, F. Beuschlein, M. Volante, C. Hantel, E. Lalli, I. Mus-Veteau, Targeting the multidrug transporter Patched potentiates chemotherapy efficiency on adrenocortical carcinoma in vitro and in vivo, *Int. J. Cancer.* 143 (2018) 199–211. <https://doi.org/10.1002/ijc.31296>.
- [41] A. Hasanovic, M. Simsir, F.S. Choveau, E. Lalli, I. Mus-Veteau, Astemizole sensitizes adrenocortical carcinoma cells to doxorubicin by inhibiting patched drug efflux activity, *Biomedicines.* 8 (2020). <https://doi.org/10.3390/BIOMEDICINES8080251>.
- [42] M.G.V. Heiden, L.C. Cantley, C.B. Thompson, Understanding the warburg effect: The metabolic requirements of cell proliferation, *Science* (80-.). 324 (2009) 1029–1033. <https://doi.org/10.1126/science.1160809>.
- [43] S.A. Hollingsworth, R.O. Dror, Molecular Dynamics Simulation for All, *Neuron.* 99 (2018) 1129–1143. <https://doi.org/10.1016/j.neuron.2018.08.011>.

- [44] J. Hrbek, J. Macáková, S. Komenda, A. Siroká, M. Rypka, On acute effects of some drugs on the higher nervous activity in man (the acoustic analyser). Clorotepin (0.5 mg and 1.0 mg), pemoline (100 mg). Part LI., *Acta Univ. Palacki. Olomuc. Fac. Med.* 111 (1985) 139–53. <https://www.ncbi.nlm.nih.gov/pubmed/2949494>.
- [45] J. Hu, Z. Liu, D.J. Yu, Y. Zhang, LS-align: An atom-level, flexible ligand structural alignment algorithm for high-throughput virtual screening, *Bioinformatics.* 34 (2018) 2209–2218. <https://doi.org/10.1093/bioinformatics/bty081>.
- [46] M. Hu, F. Yang, Y. Huang, X. You, D. Liu, S. Sun, S.-F. Sui, Structural insights into the mechanism of human NPC1L1-mediated cholesterol uptake, *Sci. Adv.* 7 (2021). <https://doi.org/10.1126/sciadv.abg3188>.
- [47] J. Huxley, *Biological Aspects of Cancer*, New York, 1958.
- [48] S. Im, H. Joo, *Ca Dojke*, (2013) 116–123.
- [49] M. ISHIKAWA, R. FUJITA, M. TAKAYANAGI, Y. TAKAYANAGI, K. SASAKI, Reversal of Acquired Resistance to Doxorubicin in K562 Human Leukemia Cells by Astemizole., *Biol. Pharm. Bull.* 23 (2000) 112–115. <https://doi.org/10.1248/bpb.23.112>.
- [50] J. Jehle, P.A. Schweizer, H.A. Katus, D. Thomas, Novel roles for hERG K + channels in cell proliferation and apoptosis, *Cell Death Dis.* 2 (2011) 1–8. <https://doi.org/10.1038/cddis.2011.77>.
- [51] K.S. Jeng, C.J. Jeng, W.J. Jeng, I.S. Sheen, S.Y. Li, C.M. Leu, Y.G. Tsay, C.F. Chang, Sonic Hedgehog signaling pathway as a potential target to inhibit the progression of hepatocellular carcinoma (Review), *Oncol. Lett.* 18 (2019) 4377–4384. <https://doi.org/10.3892/ol.2019.10826>.
- [52] K.S. Jeng, I.S. Sheen, W.J. Jeng, C.C. Lin, C.K. Lin, J.C. Su, M.C. Yu, H.Y. Fang, High expression of patched homolog-1 messenger RNA and glioma-associated oncogene-1 messenger RNA of sonic hedgehog signaling pathway indicates a risk of postresection recurrence of hepatocellular carcinoma, *Ann. Surg. Oncol.* 20 (2013) 464–473. <https://doi.org/10.1245/s10434-012-2593-y>.
- [53] K.S. Jeng, I.S. Sheen, W.J. Jeng, M.C. Yu, H.I. Hsiau, F.Y. Chang, High expression of Sonic Hedgehog signaling pathway genes indicates a risk of recurrence of breast carcinoma, *Onco. Targets. Ther.* (2013). <https://doi.org/10.2147/OTT.S54702>.
- [54] K.S. Jeng, I.S. Sheen, C.M. Leu, P.H. Tseng, C.F. Chang, The role of smoothed in cancer, *Int. J. Mol. Sci.* 21 (2020) 1–20. <https://doi.org/10.3390/ijms21186863>.
- [55] B.E. Johnson, T. Mazor, C. Hong, M. Barnes, K. Aihara, C.Y. McLean, S.D. Fouse, S. Yamamoto, H. Ueda, K. Tatsuno, S. Asthana, L.E. Jalbert, S.J. Nelson, A.W. Bollen, W.C. Gustafson, E. Charron, W.A. Weiss, I. V. Smirnov, J.S. Song, A.B. Olshen, S. Cha, Y. Zhao, R.A. Moore, A.J. Mungall, S.J.M. Jones, M. Hirst, M.A. Marra, N. Saito, H. Aburatani, A. Mukasa, M.S. Berger, S.M. Chang, B.S. Taylor, J.F. Costello, Mutational Analysis Reveals the Origin and Therapy-Driven Evolution of Recurrent Glioma, *Science* (80-.). 343 (2014) 189–193. <https://doi.org/10.1126/science.1239947>.
- [56] G. Jones, P. Willett, R.C. Glen, A.R. Leach, R. Taylor, Development and validation of a genetic algorithm for flexible docking 1 Edited by F. E. Cohen, *J. Mol. Biol.* 267 (1997) 727–748. <https://doi.org/10.1006/jmbi.1996.0897>.

- [57] J. Jumper, R. Evans, A. Pritzel, T. Green, M. Figurnov, O. Ronneberger, K. Tunyasuvunakool, R. Bates, A. Žídek, A. Potapenko, A. Bridgland, C. Meyer, S.A.A. Kohl, A.J. Ballard, A. Cowie, B. Romera-Paredes, S. Nikolov, R. Jain, J. Adler, T. Back, S. Petersen, D. Reiman, E. Clancy, M. Zielinski, M. Steinegger, M. Pacholska, T. Berghammer, S. Bodenstein, D. Silver, O. Vinyals, A.W. Senior, K. Kavukcuoglu, P. Kohli, D. Hassabis, Highly accurate protein structure prediction with AlphaFold, *Nature*. 596 (2021) 583–589. <https://doi.org/10.1038/s41586-021-03819-2>.
- [58] R.J. Kathawala, P. Gupta, C.R. Ashby, Z.S. Chen, The modulation of ABC transporter-mediated multidrug resistance in cancer: A review of the past decade, *Drug Resist. Updat.* 18 (2015) 1–17. <https://doi.org/10.1016/j.drup.2014.11.002>.
- [59] S. Kovachka, G. Mallocci, A.V. Vargiu, S. Azoulay, I. Mus-Veteau, P. Ruggerone, Molecular insights into the Patched1 drug efflux inhibitory activity of panicein A hydroquinone: a computational study, *Phys. Chem. Chem. Phys.* 23 (2021) 8013–8022. <https://doi.org/10.1039/d0cp05719c>.
- [60] N. Kumar, C.C. Su, T.H. Chou, A. Radhakrishnan, J.A. Delmar, K.R. Rajashankar, E.W. Yu, Crystal structures of the Burkholderia multivorans hopanoid transporter HpnN, *Proc. Natl. Acad. Sci. U. S. A.* 114 (2017) 6557–6562. <https://doi.org/10.1073/pnas.1619660114>.
- [61] A. Laio, M. Parrinello, Escaping free-energy minima, (2002).
- [62] Y. Liang, L. Yang, J. Xie, The Role of the Hedgehog Pathway in Chemoresistance of Gastrointestinal Cancers, *Cells*. 10 (2021) 2030. <https://doi.org/10.3390/cells10082030>.
- [63] M. V. Liberti, J.W. Locasale, The Warburg Effect: How Does it Benefit Cancer Cells?, *Trends Biochem. Sci.* 41 (2016) 211–218. <https://doi.org/10.1016/j.tibs.2015.12.001>.
- [64] Y. Liu, R.M. Huber, R. Kiefl, A. Tufman, D. Kauffmann-Guerrero, Hedgehog pathway activation might mediate pemetrexed resistance in NSCLC cells, *Anticancer Res.* 40 (2020) 1451–1458. <https://doi.org/10.21873/anticancer.14087>.
- [65] T. Long, X. Qi, A. Hassan, Q. Liang, J.K. De Brabander, X. Li, Structural basis for itraconazole-mediated NPC1 inhibition, *Nat. Commun.* 11 (2020) 1–11. <https://doi.org/10.1038/s41467-019-13917-5>.
- [66] X. Lu, Z. Wang, H. Huang, H. Wang, Hedgehog signaling promotes multidrug resistance by regulation of ABC transporters in oral squamous cell carcinoma, *J. Oral Pathol. Med.* 49 (2020) 897–906. <https://doi.org/10.1111/jop.13050>.
- [67] A.T. McNutt, P. Francoeur, R. Aggarwal, T. Masuda, R. Meli, M. Ragoza, J. Sunseri, D.R. Koes, GNINA 1.0: molecular docking with deep learning, *J. Cheminform.* 13 (2021) 1–20. <https://doi.org/10.1186/s13321-021-00522-2>.
- [68] J. Mehla, G. Mallocci, R. Mansbach, C.A. López, R. Tsivkovski, K. Haynes, I. V. Leus, S.B. Grindstaff, R.H. Cascella, N. D’cunha, L. Herndon, N.W. Hengartner, E. Margiotta, A. Atzori, A. V. Vargiu, P.D. Manrique, J.K. Walker, O. Lomovskaya, P. Ruggerone, S. Gnanakaran, V. V. Rybenkov, H.I. Zgurskaya, Predictive rules of efflux inhibition and avoidance in pseudomonas aeruginosa, *MBio.* 12 (2021) 1–19. <https://doi.org/10.1128/mBio.02785-20>.
- [69] B. Mohelnikova-Duchonova, M. Kocik, B. Duchonova, V. Brynychova, M. Oliverius, J. Hlavsa,

- E. Honsova, J. Mazanec, Z. Kala, I. Ojima, D.J. Hughes, J.E. Doherty, H.A. Murray, M.A. Crockard, R. Lemstrova, P. Soucek, Hedgehog pathway overexpression in pancreatic cancer is abrogated by new-generation taxoid SB-T-1216, *Pharmacogenomics J.* 17 (2017) 452–460. <https://doi.org/10.1038/tpj.2016.55>.
- [70] M. Mikubo, Y. Inoue, G. Liu, M.-S. Tsao, Mechanism of Drug Tolerant Persister Cancer Cells: The Landscape and Clinical Implication for Therapy, *J. Thorac. Oncol.* 16 (2021) 1798–1809. <https://doi.org/10.1016/j.jtho.2021.07.017>.
- [71] A. Momeni-Boroujeni, N. Mohammad, R. Wolber, S. Yip, M. Köbel, B.C. Dickson, M.L. Hensley, M.M. Leitao, C.R. Antonescu, R. Benayed, M. Ladanyi, C.H. Lee, S. Chiang, Targeted RNA expression profiling identifies high-grade endometrial stromal sarcoma as a clinically relevant molecular subtype of uterine sarcoma, *Mod. Pathol.* 34 (2021) 1008–1016. <https://doi.org/10.1038/s41379-020-00705-6>.
- [72] M.A. Monachon, W.P. Burkard, M. Jalfre, W. Haefely, Blockade of central 5-hydroxytryptamine receptors by methiothepin, *Naunyn. Schmiedeberg's Arch. Pharmacol.* 274 (1972) 192–197. <https://doi.org/10.1007/BF00501854>.
- [73] S. Murakami, R. Nakashima, E. Yamashita, T. Matsumoto, A. Yamaguchi, Crystal structures of a multidrug transporter reveal a functionally rotating mechanism, *Nature.* 443 (2006) 173–179. <https://doi.org/10.1038/nature05076>.
- [74] H. Nikaido, RND transporters in the living world, *Res. Microbiol.* 169 (2018) 363–371. <https://doi.org/10.1016/j.resmic.2018.03.001>.
- [75] T. Ozben, Mechanisms and strategies to overcome multiple drug resistance in cancer, *FEBS Lett.* 580 (2006) 2903–2909. <https://doi.org/10.1016/j.febslet.2006.02.020>.
- [76] N.S. Pagadala, K. Syed, J. Tuszynski, Software for molecular docking: a review, *Biophys. Rev.* 9 (2017) 91–102. <https://doi.org/10.1007/s12551-016-0247-1>.
- [77] K. Petrov, B.M. Wierbowski, J. Liu, A. Salic, Distinct Cation Gradients Power Cholesterol Transport at Different Key Points in the Hedgehog Signaling Pathway, *Dev. Cell.* 55 (2020) 314–327.e7. <https://doi.org/10.1016/j.devcel.2020.08.002>.
- [78] J.W. Ponder, C. Wu, P. Ren, V.S. Pande, J.D. Chodera, M.J. Schnieders, I. Haque, D.L. Mobley, D.S. Lambrecht, R.A. Distasio, M. Head-Gordon, G.N.I. Clark, M.E. Johnson, T. Head-Gordon, Current status of the AMOEBA polarizable force field, *J. Phys. Chem. B.* 114 (2010) 2549–2564. <https://doi.org/10.1021/jp910674d>.
- [79] M. Prieto-Vila, R.U. Takahashi, W. Usuba, I. Kohama, T. Ochiya, Drug resistance driven by cancer stem cells and their niche, *Int. J. Mol. Sci.* 18 (2017). <https://doi.org/10.3390/ijms18122574>.
- [80] C. Qi, G. Di Minin, I. Vercellino, A. Wutz, V.M. Korkhov, Structural basis of sterol recognition by human hedgehog receptor PTCH1, *Sci. Adv.* 5 (2019) 1–9. <https://doi.org/10.1126/sciadv.aaw6490>.
- [81] X. Qi, P. Schmiedege, E. Coutavas, X. Li, Two patched molecules engage distinct sites on hedgehog yielding a signaling-competent complex, *Science* (80-.). 362 (2018). <https://doi.org/10.1126/science.aas8843>.

- [82] X. Qi, P. Schmiede, E. Coutavas, J. Wang, X. Li, Structures of human Patched and its complex with native palmitoylated sonic hedgehog, *Nature*. 560 (2018) 128–132. <https://doi.org/10.1038/s41586-018-0308-7>.
- [83] H. Qian, P. Cao, M. Hu, S. Gao, N. Yan, X. Gong, Inhibition of tetrameric Patched1 by Sonic Hedgehog through an asymmetric paradigm, *Nat. Commun.* 10 (2019). <https://doi.org/10.1038/s41467-019-10234-9>.
- [84] A. Radhakrishnan, R. Rohatgi, C. Siebold, Cholesterol access in cellular membranes controls Hedgehog signaling, *Nat. Chem. Biol.* 16 (2020) 1303–1313. <https://doi.org/10.1038/s41589-020-00678-2>.
- [85] S. Raschka, B. Kaufman, Machine learning and AI-based approaches for bioactive ligand discovery and GPCR-ligand recognition, *Methods*. 180 (2020) 89–110. <https://doi.org/10.1016/j.ymeth.2020.06.016>.
- [86] E. Reading, Z. Ahdash, C. Fais, V. Ricci, X. Wang-Kan, E. Grimsey, J. Stone, G. Mallocci, A.M. Lau, H. Findlay, A. Konijnenberg, P.J. Booth, P. Ruggerone, A. V. Vargiu, L.J.V. Piddock, A. Politis, Perturbed structural dynamics underlie inhibition and altered efflux of the multidrug resistance pump AcrB, *Nat. Commun.* 11 (2020). <https://doi.org/10.1038/s41467-020-19397-2>.
- [87] S.K. Riaz, J.S. Khan, S.T.A. Shah, F. Wang, L. Ye, W.G. Jiang, M.F.A. Malik, Involvement of hedgehog pathway in early onset, aggressive molecular subtypes and metastatic potential of breast cancer, *Cell Commun. Signal.* 16 (2018) 1–12. <https://doi.org/10.1186/s12964-017-0213-y>.
- [88] M.F. Richter, B.S. Drown, A.P. Riley, A. Garcia, T. Shirai, R.L. Svec, P.J. Hergenrother, Predictive compound accumulation rules yield a broad-spectrum antibiotic, *Nature*. 545 (2017) 299–304. <https://doi.org/10.1038/nature22308>.
- [89] S. Riniker, J.R. Allison, W.F. Van Gunsteren, On developing coarse-grained models for biomolecular simulation: A review, *Phys. Chem. Chem. Phys.* 14 (2012) 12423–12430. <https://doi.org/10.1039/c2cp40934h>.
- [90] R.W. Robey, K.M. Pluchino, M.D. Hall, A.T. Fojo, S.E. Bates, M.M. Gottesman, Revisiting the role of ABC transporters in multidrug-resistant cancer, *Nat. Rev. Cancer*. 18 (2018) 452–464. <https://doi.org/10.1038/s41568-018-0005-8>.
- [91] A.F. Rudolf, M. Kinnebrew, C. Kowatsch, T.B. Ansell, K. El Omari, B. Bishop, E. Pardon, R.A. Schwab, T. Malinauskas, M. Qian, R. Duman, D.F. Covey, J. Steyaert, A. Wagner, M.S.P. Sansom, R. Rohatgi, C. Siebold, The morphogen Sonic hedgehog inhibits its receptor Patched by a pincer grasp mechanism, *Nat. Chem. Biol.* 15 (2019) 975–982. <https://doi.org/10.1038/s41589-019-0370-y>.
- [92] O.M.H. Salo-ahen, I. Alanko, R. Bhadane, A.M.J.J. Bonvin, R.V. Honorato, S. Hossain, A.H. Juffer, A. Kabedev, M. Lahtela-kakkonen, A.S. Larsen, E. Lescrinier, P. Marimuthu, and Pharmaceutical Development, (2021) 1–60.
- [93] Z. Saze, M. Terashima, M. Kogure, F. Ohsuka, H. Suzuki, M. Gotoh, Activation of the sonic hedgehog pathway and its prognostic impact in patients with gastric cancer, *Dig. Surg.* 29 (2012)

- 115–123. <https://doi.org/10.1159/000336949>.
- [94] S.J. Scales, F.J. de Sauvage, Mechanisms of Hedgehog pathway activation in cancer and implications for therapy, *Trends Pharmacol. Sci.* (2009). <https://doi.org/10.1016/j.tips.2009.03.007>.
- [95] J. Schlitter, M. Engels, P. Krüger, Targeted molecular dynamics: A new approach for searching pathways of conformational transitions, *J. Mol. Graph.* 12 (1994) 84–89. [https://doi.org/10.1016/0263-7855\(94\)80072-3](https://doi.org/10.1016/0263-7855(94)80072-3).
- [96] L. Signetti, N. Elizarov, M. Simsir, A. Paquet, D. Douguet, F. Labbal, D. Debayle, A. Di Giorgio, V. Biou, C. Girard, M. Duca, L. Bretillon, C. Bertolotto, B. Verrier, S. Azoulay, I. Mus-Veteau, Inhibition of patched drug efflux increases vemurafenib effectiveness against resistant brafv600e melanoma, *Cancers (Basel)*. (2020). <https://doi.org/10.3390/cancers12061500>.
- [97] A.N. Sigafos, B.D. Paradise, M.E. Fernandez-Zapico, Hedgehog/GLI Signaling Pathway: Transduction, Regulation, and Implications for Disease, *Cancers (Basel)*. 13 (2021) 3410. <https://doi.org/10.3390/cancers13143410>.
- [98] M. Simsir, I. Mus-Veteau, RND family efflux pumps: from antibioresistance to chemotherapy resistance, *Swedish J. Biosci. Res.* 1 (2020) 51–61. <https://doi.org/10.51136/sjbsr.2020.51.61>.
- [99] H. Sjuets, A. V. Vargiu, S.M. Kwasny, S.T. Nguyen, H.S. Kim, X. Ding, A.R. Ornik, P. Ruggerone, T.L. Bowlin, H. Nikaido, K.M. Pos, T.J. Opperman, Molecular basis for inhibition of AcrB multidrug efflux pump by novel and powerful pyranopyridine derivatives, *Proc. Natl. Acad. Sci. U. S. A.* 113 (2016) 3509–3514. <https://doi.org/10.1073/pnas.1602472113>.
- [100] Y. Sugita, Y. Okamoto, Replica-exchange molecular dynamics method for protein folding, *Chem. Phys. Lett.* 314 (1999) 141–151. [https://doi.org/10.1016/S0009-2614\(99\)01123-9](https://doi.org/10.1016/S0009-2614(99)01123-9).
- [101] H. Sung, J. Ferlay, R.L. Siegel, M. Laversanne, I. Soerjomataram, A. Jemal, F. Bray, Global Cancer Statistics 2020: GLOBOCAN Estimates of Incidence and Mortality Worldwide for 36 Cancers in 185 Countries, *CA. Cancer J. Clin.* 71 (2021) 209–249. <https://doi.org/10.3322/caac.21660>.
- [102] H-K. Tam, V.N. Malviya, W-E. Foong, A. Herrmann, G. Mallocci, P. Ruggerone, A.V. Vargiu, and K.M. Pos. Binding and transport of carboxylated drugs by the multidrug transporter acrb. *Journal of Molecular Biology*, 432 (2020) 861–877.
- [103] L.P. Tangella, M. Arooj, E. Deplazes, E.S. Gray, R.L. Mancera, Identification and characterisation of putative drug binding sites in human ATP-binding cassette B5 (ABCB5) transporter, *Comput. Struct. Biotechnol. J.* 19 (2021) 691–704. <https://doi.org/10.1016/j.csbj.2020.12.042>.
- [104] O. Trott, A.J. Olson, AutoDock Vina: Improving the speed and accuracy of docking with a new scoring function, efficient optimization, and multithreading, *J. Comput. Chem.* (2009). <https://doi.org/10.1002/jcc.21334>.
- [105] K. Tunyasuvunakool, J. Adler, Z. Wu, T. Green, M. Zielinski, A. Židek, A. Bridgland, A. Cowie, C. Meyer, A. Laydon, S. Velankar, G.J. Kleywegt, A. Bateman, R. Evans, A. Pritzel, M. Figurnov, O. Ronneberger, R. Bates, S.A.A. Kohl, A. Potapenko, A.J. Ballard, B. Romera-

- Paredes, S. Nikolov, R. Jain, E. Clancy, D. Reiman, S. Petersen, A.W. Senior, K. Kavukcuoglu, E. Birney, P. Kohli, J. Jumper, D. Hassabis, Highly accurate protein structure prediction for the human proteome, *Nature*. 596 (2021) 590–596. <https://doi.org/10.1038/s41586-021-03828-1>.
- [106] M.W. Van Der Kamp, A.J. Mulholland, Combined quantum mechanics/molecular mechanics (QM/MM) methods in computational enzymology, *Biochemistry*. 52 (2013) 2708–2728. <https://doi.org/10.1021/bi400215w>.
- [107] M.L. Verdonk, J.C. Cole, M.J. Hartshorn, C.W. Murray, R.D. Taylor, Improved protein-ligand docking using GOLD, *Proteins Struct. Funct. Genet.* 52 (2003) 609–623. <https://doi.org/10.1002/prot.10465>.
- [108] J.Q. Wang, Y. Yang, C.Y. Cai, Q.X. Teng, Q. Cui, J. Lin, Y.G. Assaraf, Z.S. Chen, Multidrug resistance proteins (MRPs): Structure, function and the overcoming of cancer multidrug resistance, *Drug Resist. Updat.* 54 (2021) 100743. <https://doi.org/10.1016/j.drug.2021.100743>.
- [109] H. Xie, B.D. Paradise, W.W. Ma, M.E. Fernandez-zapico, Recent Advances in the Clinical Targeting of, *Cell Prolif.* 8 (2019) 1–17.
- [110] X. Xu, H. Ding, G. Rao, S. Arora, C.P. Saclarides, J. Esparaz, P. Gattuso, C.C. Solorzano, R.A. Prinz, Activation of the Sonic Hedgehog pathway in thyroid neoplasms and its potential role in tumor cell proliferation, *Endocr. Relat. Cancer.* 19 (2012) 167–179. <https://doi.org/10.1530/ERC-11-0305>.
- [111] B. Yu, D. Gu, X. Zhang, J. Li, B. Liu, J. Xie, GLI1-mediated regulation of side population is responsible for drug resistance in gastric cancer, *Oncotarget.* 8 (2017) 27412–27427. <https://doi.org/10.18632/oncotarget.16174>.
- [112] Y. Zhang, D.P. Bulkley, Y. Xin, K.J. Roberts, D.E. Asarnow, A. Sharma, B.R. Myers, W. Cho, Y. Cheng, P.A. Beachy, Structural Basis for Cholesterol Transport-like Activity of the Hedgehog Receptor Patched, *Cell.* 175 (2018) 1352-1364.e14. <https://doi.org/10.1016/j.cell.2018.10.026>.
- [113] R. Zhou, Replica exchange molecular dynamics method for protein folding simulation., *Methods Mol. Biol.* 350 (2007) 205–223. <https://doi.org/10.1385/1-59745-189-4:205>.
- [114] W. Zhu, Z. You, T. Li, C. Yu, G. Tao, M. Hu, X. Chen, Correlation of hedgehog signal activation with chemoradiotherapy sensitivity and survival in esophageal squamous cell carcinomas, *Jpn. J. Clin. Oncol.* 41 (2011) 386–393. <https://doi.org/10.1093/jjco/hyq217>.